

## Research Article

Selected Paper from the 11th Pure and Applied Chemistry International Conference 2017 (PACCON 2017)

**Hydrogen-Rich Syngas Production from Biogas Reforming by Gliding Arc Plasma-Catalyst Minireactor**

Banhan Khanchai and Nongnuch Rueangjitt\*

Department of Industrial Chemistry, Faculty of Science, Chiang Mai University, Chiang Mai, Thailand

Sumaeth Chavadej

The Petroleum and Petrochemical College, Chulalongkorn University, Thailand

Hidetoshi Sekiguchi

Department of Chemical Engineering, Faculty of Engineering, Tokyo Institute of Technology, Japan

\* Corresponding author. E-mail: nongnuch.r@cmu.ac.th

DOI: 10.14416/j.ijast.2017.11.002

Received: 14 June 2017; Accepted: 27 July 2017; Published online: 24 November 2017

© 2017 King Mongkut's University of Technology North Bangkok. All Rights Reserved.

**Abstract**

This research aim was to investigate the production of H<sub>2</sub>-rich syngas from simulated biogas waste using a developed gliding arc plasma minireactor integrated with nickel-based catalysts. The effect of different catalyst types of NiO/Al<sub>2</sub>O<sub>3</sub>, NiO/MS 5A and NiO/ZSM-5 zeolite on overall system performance was investigated. Different support types significantly affected physical and chemical properties of prepared catalyst and had the dominant roles on the biogas plasma reforming in different ways. The integration of NiO/Al<sub>2</sub>O<sub>3</sub> catalysts into gliding arc plasma minireactor gave the remarkable enhancement of H<sub>2</sub> product in syngas with high H<sub>2</sub> selectivity and H<sub>2</sub>/CO molar ratio of 63.59% and 2.91, respectively. Using NiO/Al<sub>2</sub>O<sub>3</sub> catalyst in this plasma system lead the synergistic effect on H<sub>2</sub> selectivity, as compared the only plasma system. NiO/ZSM-5 catalyst provided the highest CH<sub>4</sub> conversion of 19.29% and also gave the minimum consumed energy of system ( $E_c=6.14 \times 10^{-18}$  W·s/molecule of biogas converted and  $E_s=5.52 \times 10^{-18}$  W·s/molecule of syngas produced). The gliding arc plasma minireactor of this work performed the biogas reforming better than other low-temperature plasma such as conventional dielectric barrier discharge system.

**Keywords:** Biogas reforming, Syngas, Gliding Arc Discharge, Plasma

**1 Introduction**

Nowadays, many researches have been focused to reduce CO<sub>2</sub> and CH<sub>4</sub> greenhouse gases, which caused a big problem concerning global warming effect. Biogas is one of greenhouse gas routes which generated via anaerobic digestion of organic waste. In general, biogas waste mainly consists of CH<sub>4</sub> (55–70%), CO<sub>2</sub> (30–45%) and traces of other gases [1]. Biogas can be widely used as a fuel source including

for heating or lighting applications, and to power combustion engines for electricity generation. Nevertheless, an addition of CO<sub>2</sub> separation unit before use is necessarily required because high CO<sub>2</sub> content lead to lower the heating value of fuel. CO<sub>2</sub> emission from separation causes the increasing greenhouse effect problem. Hence, researches have been brought these two gases (CO<sub>2</sub> and CH<sub>4</sub>) to utilize and to upgrade the value. Syngas production from gases containing CH<sub>4</sub> and CO<sub>2</sub> is an interesting

Please cite this article as: B. Khanchai, S. Chavadej, H. Sekiguchi, and N. Rueangjitt, "Hydrogen-rich syngas production from biogas reforming by Gliding Arc Plasma-Catalyst minireactor," *KMUTNB Int J Appl Sci Technol*, vol. 10, no. 4, pp. 279–285, Oct.–Dec. 2017.

route. Since syngas is a gas mixture having primarily of hydrogen ( $H_2$ ) and carbon monoxide (CO), which can be used as raw materials for producing various chemicals such as methanol, ammonia, formaldehyde and synthetic liquid fuel via Fischer-Tropsch process. Especially for  $H_2$ , it can be used as fuel for generating electricity [2]. The process widely used in the industry for syngas production is steam reforming process [3]–[5]. Also,  $CO_2$  reforming of methane or Dry Methane Reforming (DMR) is another one of reforming processes for syngas production.



However, this process still has the problems i.e. operation at high temperature and pressure, slow response time and catalyst deactivation. Low-temperature plasma technology is very interesting ones which can be applied in syngas production because it can activate the reaction to occur at ambient temperature and atmospheric pressure. Also, the reaction has fast response time [2]. Under applying a high voltage plasma system, gas phase is broken down to form highly reactive species of electrons, highly excited atoms and molecules (ions, radicals, photons and neutral particles). The collisions between these highly energetic species enable reactions to proceed within plasma [5]. There are several types of low-temperature plasma used for various chemical reactions including microwave discharge, corona discharge, spark discharge, dielectric barrier discharge and gliding arc discharge. Gliding arc discharge is considered an ideal technique for conversion of hydrocarbons because it provides a high energy density discharge with a relatively low bulk gas temperature [6]. Moreover, a number of papers [7]–[10] reported that a combination of low-temperature plasma technology with catalyst can enhance reactant conversion, product distribution and consumed energy. In our previous work [7], we have successfully employed the designed mini-Gliding Arc Discharge (GAD) reactor for investigating the non-oxidative methane reforming with Ni loaded on porous silica-alumina plate. Thus, this research continued to develop the configuration of GAD plasma-catalyst minireactor for biogas reforming study, with concerning the integration of different catalyst support types with gliding arc discharge plasma.

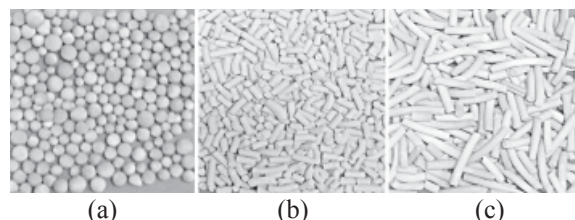


**Figure 1:** Photographs of prepared catalysts (a)  $NiO/Al_2O_3$ , (b)  $NiO/MS\ 5A$  and (c)  $NiO/ZSM-5$ .

## 2 Materials and Methods

### 2.1 Catalyst preparation

5% wt. of NiO loaded on three different catalyst supports (alumina bead, molecular sieve 5A pellet and ZSM-5 zeolite pellet) were prepared by incipient wetness impregnation method with using  $NiNO_3$  aqueous solution as a metal precursor.  $Al_2O_3$  bead was supplied by Fluka Chemical Corp., Molecular Sieve 5A° or MS 5A pellet was supplied by Sigma-Aldrich Corp. and ZSM-5 zeolite ( $Si/Al=60$ ) pellet was supplied by Hutong Global (China) Co., Ltd. Firstly, the proper amount of  $Ni(NO_3)_2 \cdot 6H_2O$  (QRéC Chemical Co., Ltd.) was dissolved in the sufficient deionized water, and then the  $NiNO_3$  solution was slowly dropped on supports. After impregnation, all catalysts were dried overnight at 110°C and calcined in air at 500°C for 5 h. Figure 1(a)–(c) illustrated the sample of prepared catalysts i.e.  $NiO/Al_2O_3$ ,  $NiO/MS\ 5A$  and  $NiO/ZSM-5$ .

### 2.2 Catalyst characterization

Catalyst samples were characterized by surface area analyzer (Autosorb-1 MP, Quantachrome) and Scanning Electron Microscope equipped with Energy Dispersive Spectrometer (SEM-EDS, JEOL JSM-IT300LV), in order to correlate physical and chemical characteristics with catalytic properties. Specific surface area, total pore volume and average pore radius of unloaded and loaded catalysts on three kinds of support were determined by  $N_2$  adsorption using Brunauer-Emmett-Teller (BET) method. Surface morphology of catalysts was identified by SEM, and elemental distribution on catalyst sample surface was analyzed by EDS.

### 2.3 Catalytic plasma reforming testing

Experimental setup of GAD plasma system for biogas reforming testing under catalytic-plasma condition was shown in Figure 2. The developed GAD plasma-catalyst minireactor which was shown in Figure 3 was made of two acrylic plates as reactor wall, with a width of 10.5 cm, a length of 13.5 cm, an outside thickness of 1.5 cm, and an inside thickness of 0.5 cm [7]. There were two diverging curve-shaped electrodes, made from stainless steel sheet with a thickness of 1.5 mm and electrode gap distance of 4.5 cm. A rubber sheet was placed between lower acrylic plate and electrode sheet on both sides to seal the reactor. Feed gas ( $\text{CH}_4:\text{CO}_2$  of 70:30), supplied by Linde Co., Ltd., was introduced into GAD minireactor. Solid catalyst in spherical and cylindrical shape forms was placed into a holder, made from silicone rubber sheet (width of 3 cm, length of 6 cm), and then was packed on the back side of the minireactor. The flow rate of feed gas was controlled by digital mass flow controller (New-Flow, TLFC). The soap bubble flow meter used to measure the flow rates of feed and product gas. After the composition of feed gas was invariant with time, the power supply unit was turned on. The AC power supply unit was used to generate the gliding arc discharge in the reactor. The input voltage and frequency were controlled by a function generator (GW Instek, GFG-802OH). A power analyzer (Lutron, DW6090) was used to measure power, current and output voltage. The operating condition was fixed at a feed flow rate of 25  $\text{cm}^3/\text{min}$ , an input frequency of 300 Hz, an applied voltage of 16.25 kV. The product gas was taken for composition analysis by Gas Chromatograph (HP 6890), equipped with a HP-PLOT Molecular Sieve 5A capillary column and Thermal Conductivity Detector (TCD). During the reaction, the product gas was taken at least three times for each experiment.

### 2.4 Evaluation and analysis of system performance

The biogas ( $\text{CH}_4$  or  $\text{CO}_2$ ) conversion is defined in Equation (1).

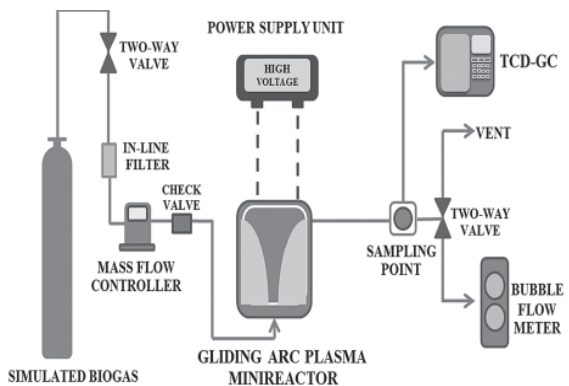


**Figure 2:** Experimental schematic of catalytic plasma reforming system.

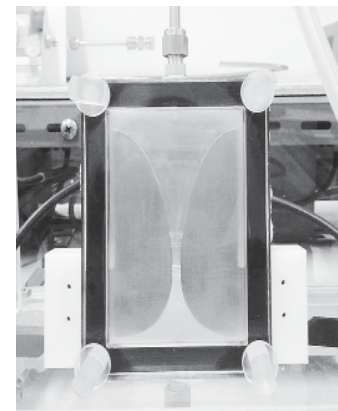


**Figure 3:** Photograph of gliding arc plasma minireactor in this work.

$$\% \text{ biogas conversion} =$$

$$\frac{(\text{moles of biogas in} - \text{moles of biogas out})(100)}{(\text{moles of biogas in})} \quad (1)$$

The selectivity for syngas ( $\text{H}_2$  and  $\text{CO}$ ) is calculated based on moles of H-containing reactant ( $\text{CH}_4$ ) converted as stated in Equation (2) and moles of C-containing reactant ( $\text{CH}_4$  and  $\text{CO}_2$ ) converted, as stated in Equation (3), respectively. Also,  $\text{H}_2/\text{CO}$  molar ratio is defined in Equation (4).

$$\% \text{H}_2 \text{ selectivity} = \frac{(\text{moles of H}_2 \text{ produced})(100)}{(2 \times \text{moles of CH}_4 \text{ converted})} \quad (2)$$

% CO selectivity =

$$\frac{(\text{moles of CO produced}) (100)}{(\text{moles of CH}_4 \text{ converted} + \text{moles of CO}_2 \text{ converted})} \quad (3)$$

$$\text{H}_2/\text{CO molar ratio} = \frac{\text{moles of H}_2 \text{ produced}}{\text{moles of CO produced}} \quad (4)$$

The specific energy consumption is calculated in a unit of W·s per biogas molecule converted or per syngas molecule produced, as stated in Equation (5).

$$\text{specific energy consumption} = (P) (60) / (N) (M) \quad (5)$$

where P = power (W), N = Avogadro's number ( $6.02 \times 10^{23}$  molecules·gmol<sup>-1</sup>), M = rate of biogas converted or of syngas produced molecules (gmol·min<sup>-1</sup>)

### 3 Results and Discussion

#### 3.1 Catalyst characterization result

Table 1 illustrated the analysis results of specific surface area, total pore volume and average pore radius by Surface Area & Pore Analyzer. It showed that the given data of three catalyst support types were comparatively different. Surface area of Al<sub>2</sub>O<sub>3</sub>, ZSM-5 and MS 5A supports (unloaded catalysts) were about 272, 249 and 18 m<sup>2</sup>/g, respectively. The surface area seemed to be not much different when NiO was loaded on support surface, except for Al<sub>2</sub>O<sub>3</sub> support. The specific surface area of NiO/Al<sub>2</sub>O<sub>3</sub> catalyst was reduced by ~100 m<sup>2</sup>/g, as compared to unloaded Al<sub>2</sub>O<sub>3</sub>. In different way, the total pore volume tended to decrease when loaded NiO on support surface for all three types of support, due to deposition of NiO crystal phase over support surface.

**Table 1:** Specific surface area, total pore volume and average pore radius of prepared catalysts

Type of Catalyst	Surface Area (m <sup>2</sup> /g)	Pore Volume (cm <sup>3</sup> /g)	Pore Radius (Å)
Al <sub>2</sub> O <sub>3</sub>	272.19	0.5646	41.48
NiO/Al <sub>2</sub> O <sub>3</sub>	170.11	0.3977	46.75
MS 5A	17.83	0.0881	98.91
NiO/MS 5A	16.72	0.0837	100.10
ZSM-5	247.69	0.2561	20.68
NiO/ZSM-5	250.25	0.2371	18.95

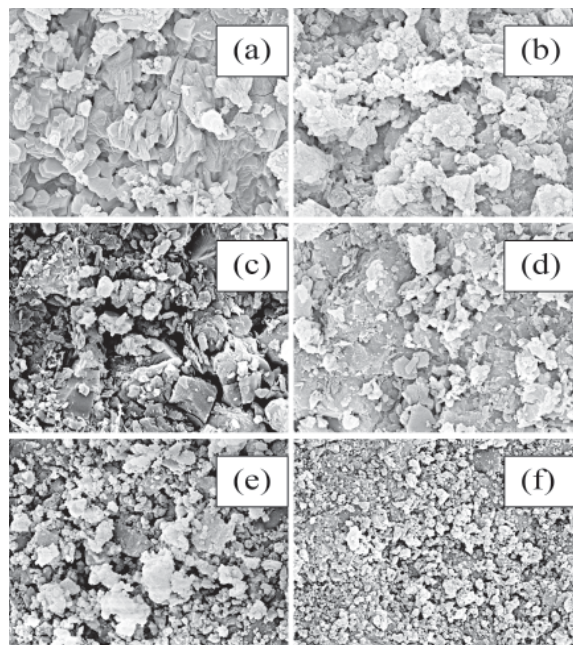


**Figure 4:** SEM micrographs of prepared catalysts (a) Al<sub>2</sub>O<sub>3</sub>, (b) NiO/Al<sub>2</sub>O<sub>3</sub>, (c) MS 5A, (d) NiO/MS 5A, (e) ZSM-5 and (f) NiO/ZSM-5.

Figure 4 (a)–(f) illustrated SEM micrographs of catalyst samples including unloaded and NiO-loaded Al<sub>2</sub>O<sub>3</sub>, MS 5A and ZSM-5 catalysts. It is clearly seen that surface morphology of NiO-loaded catalysts had difference from ones of unloaded catalyst, implying NiO could be deposited on support surface. Figure 5 (a)–(c) showed SEM micrographs and EDS area mappings of Ni element on different NiO-loaded catalysts. It found that the dispersion of Ni element over MS 5A surface was highest while NiO/ZSM-5 appeared the lowest dispersion of Ni element. It indicated that different types of catalyst support significantly affected the dispersion of Ni element.

Table 2 presented the quantitative elemental analysis results from EDS technique. The percentage of weight and atomic weight of Ni element on all NiO-loaded catalyst surface were in a range from about 6 to 10%, and from 2 to 4%, respectively. Nevertheless, NiO/MS 5A catalyst had the highest percent weight and atomic weight of Ni and O elements, which corresponded to the Ni dispersion result by EDS in Figure 5(b), as mentioned earlier.

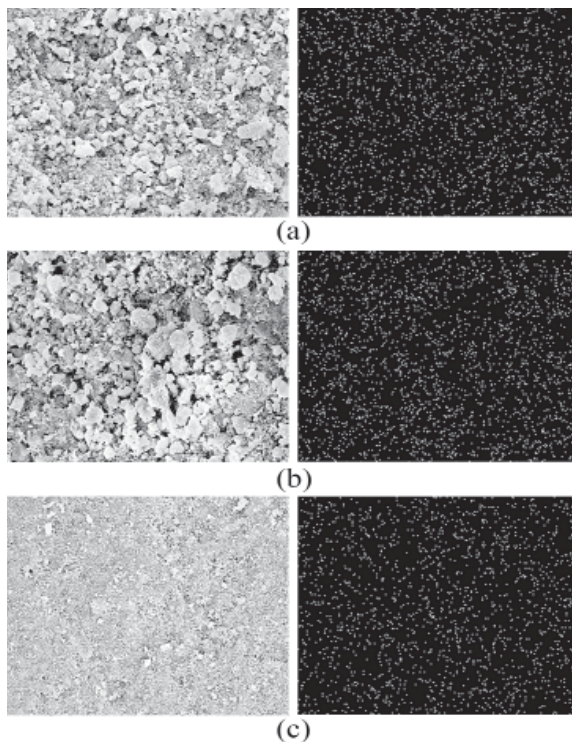


**Figure 5:** SEM micrographs and EDS area mappings of Ni element on different support catalysts (a) NiO/Al<sub>2</sub>O<sub>3</sub>, (b) NiO/MS 5A and (c) NiO/ZSM-5.

**Table 2:** Percent weight and atomic weight of Ni and O elements on different supports

Type of catalyst	Weight (%)		Atomic weight (%)	
	Ni	O	Ni	O
NiO/Al <sub>2</sub> O <sub>3</sub>	8.56	42.28	3.16	57.31
NiO/MS 5A	10.27	45.88	3.78	61.89
NiO/ZSM-5	5.57	43.03	2.04	57.88

### 3.2 Catalytic plasma biogas reforming result

In order to understand the influential role of different catalyst types on the overall performance of biogas plasma reforming and discharge behavior, a series of experiments were performed in GAD plasma-catalyst minireactor. Six types of catalyst samples including Al<sub>2</sub>O<sub>3</sub>, NiO/Al<sub>2</sub>O<sub>3</sub>, MS 5A, NiO/MS 5A, ZSM-5 and NiO/ZSM-5 were thoroughly examined in this study.

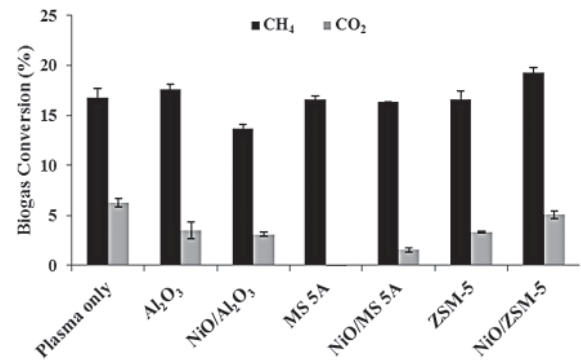


**Figure 6:** Effect of different catalyst types on biogás conversion.

#### 3.2.1 Effect of different catalyst types on biogas conversion

Figure 6 illustrated the effect of different catalyst types on CH<sub>4</sub> and CO<sub>2</sub> conversions. The result showed that when using unloaded Al<sub>2</sub>O<sub>3</sub> and NiO/ZSM-5, the obtained values of CH<sub>4</sub> conversion were greater than the only plasma system (no catalyst) while NiO/Al<sub>2</sub>O<sub>3</sub> provided the less ones. For MS 5A, NiO/MS 5A and ZSM-5, CH<sub>4</sub> conversion seemed to be close with the only plasma system. Regarding the result of CO<sub>2</sub> conversion, all types of catalyst gave lower CO<sub>2</sub> conversion than only plasma system. The lowest CO<sub>2</sub> conversion was found in MS 5A. In case of MS 5A, CO<sub>2</sub> conversion was minus value. In addition to the comparative result of CH<sub>4</sub> and CO<sub>2</sub> conversions between unloaded and NiO-loaded catalysts, it can be seen that NiO-loaded Al<sub>2</sub>O<sub>3</sub> gave CH<sub>4</sub> and CO<sub>2</sub> conversions lower than unloaded Al<sub>2</sub>O<sub>3</sub> while NiO-loaded MS 5A provided the close value of CH<sub>4</sub> conversion and lower CO<sub>2</sub> conversion, as compared to unloaded MS 5A. Herein, only ZSM-5 catalyst support exhibited the improvement of CH<sub>4</sub> and CO<sub>2</sub> conversions when loading NiO. NiO/ZSM-5 catalyst provided the highest CH<sub>4</sub> and relatively high CO<sub>2</sub> conversions of 19.29% and 5.07%, respectively.

#### 3.2.2 Effect of different catalyst types on syngas selectivity and H<sub>2</sub>/CO molar ratio

Figure 7 illustrated the effect of different catalyst types on H<sub>2</sub> and CO selectivities. It found that when

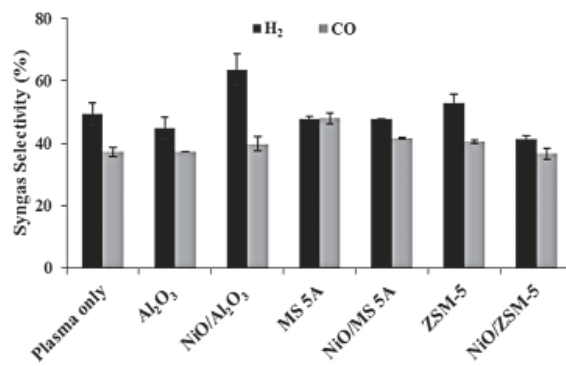


**Figure 7:** Effect of different catalyst types on syngas selectivity.

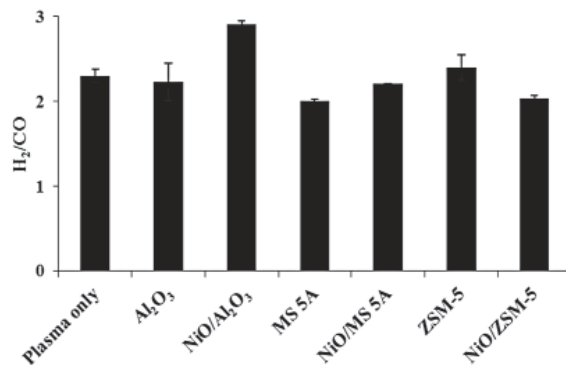


**Figure 8:** Effect of different catalyst types on H<sub>2</sub>/CO molar ratio.

using NiO/Al<sub>2</sub>O<sub>3</sub> and ZSM-5, the obtained values of H<sub>2</sub> selectivity were higher while H<sub>2</sub> selectivity was lower when using Al<sub>2</sub>O<sub>3</sub>, MS 5A, NiO/MS 5A and NiO/ZSM-5, as compared to the only plasma system. For the result of CO selectivity, CO selectivity was slightly increased from the only plasma system when using NiO/Al<sub>2</sub>O<sub>3</sub>, MS 5A, NiO/MS 5A and ZSM-5. For the comparison of H<sub>2</sub> and CO selectivities between unloaded and NiO-loaded catalysts, the result revealed that only Al<sub>2</sub>O<sub>3</sub> support could enhance these selectivities when NiO was loaded on Al<sub>2</sub>O<sub>3</sub> surface. However, H<sub>2</sub> and CO selectivities were less when using NiO/ZSM-5, as compared to unloaded ZSM-5. For MS 5A support, H<sub>2</sub> selectivity seemed to be close with unloaded MS 5A when using NiO/MS 5A, and CO selectivity was less. From the results, it indicated that, the integration of NiO/Al<sub>2</sub>O<sub>3</sub> catalyst with gliding arc discharge performed the positive

effect to syngas selectivity, especially selectivity for H<sub>2</sub>. NiO/Al<sub>2</sub>O<sub>3</sub> catalyst provided the highest H<sub>2</sub> selectivity of 63.59%. Moreover, in Figure 8, H<sub>2</sub>/CO molar ratio were in range of 2.01–2.91. Interestingly, NiO/Al<sub>2</sub>O<sub>3</sub> catalyst gave the hydrogen-rich syngas with the highest H<sub>2</sub>/CO molar ratio of 2.91.

### 3.2.3 Effect of different catalyst types on specific energy consumption

Table 3 illustrated the specific energy consumption in terms of either per molecule of biogas converted (E<sub>C</sub>) or per molecule of syngas produced (E<sub>S</sub>). The result showed that, the energy consumption per molecule of biogás converted was more required when using catalysts in this studied GAD plasma system, except for NiO/ZSM-5. The minimum E<sub>C</sub> was at 6.14x10<sup>-18</sup> W·s/molecule of biogas converted when using NiO/ZSM-5. For the result of specific energy consumption per molecule of syngas produced, both catalyst-plasma system and only plasma system provided the close value, and E<sub>S</sub> was in range of 5.51x10<sup>-18</sup>–6.11x10<sup>-18</sup> W·s/molecule of syngas produced. Similar to E<sub>C</sub>, the minimum E<sub>S</sub> was at 5.52x10<sup>-18</sup> W·s/molecule of syngas produced when using NiO/ZSM-5.

**Table 3:** Effect of different catalyst types on energy consumption

Type of Catalyst	Energy Consumption (x10 <sup>-18</sup> W·s/molecule)	
	E <sub>C</sub>	E <sub>S</sub>
No catalyst (plasma only)	7.36	5.98
Al <sub>2</sub> O <sub>3</sub>	7.35	6.11
NiO/Al <sub>2</sub> O <sub>3</sub>	8.57	5.51
MS 5A	8.75	6.07
NiO/MS 5A	8.04	6.02
ZSM-5	8.04	5.81
NiO/ZSM-5	6.14	5.52

## 4 Conclusions

This developed gliding arc discharge plasma minireactor can perform the biogas reforming for syngas production under catalyst-plasma condition. The different catalyst types have their specific effect on the overall performance of biogas reforming and

discharge behavior in different ways. The integration of NiO/Al<sub>2</sub>O<sub>3</sub> catalyst with this gliding arc discharge performed the significant changes on biogas conversion, syngas selectivity, H<sub>2</sub>/CO ratio and energy consumption, suggesting that some interaction between the two metal oxides of NiO/Al<sub>2</sub>O<sub>3</sub> catalyst might be concerned.

### Acknowledgments

This research work was financially supported under TRF Senior Research Scholar Grant No. RTA578008 and Graduate School, Chiang Mai University. The authors would like to convey special appreciation to the academic committee of Pure and Applied Chemistry International Conference (PACCON2017) for providing the opportunity for this work to be published in this journal.

### References

- [1] D. Deublein and A. Steinhauser, *Biogas from Waste and Renewable Resources: An Introduction*. Wiley-VCH, Germany, 2011, pp. 85–95.
- [2] A. Aziznia, H. R. Bozorgzadeh, N. Seyed-Matin, M. Baghalha, and A. Mohamadalizadeh, “Comparison of dry reforming of methane in low temperature hybrid plasma-catalytic corona with thermal catalytic reactor over Ni/γ-Al<sub>2</sub>O<sub>3</sub>,” *Journal of Natural Gas Chemistry*, vol. 21, no. 4, pp. 466–475, Mar. 2012.
- [3] B. Sorenen, *Hydrogen and Fuel Cell*. Oxford: Elsevier Academic Press, 2005, pp. 6–10.
- [4] J. A. Moulijn, *Chemical Process Technology*. New York: John Wiley & Sons, 2004, pp. 129–139.
- [5] R. B. Gupta, *Hydrogen fuel: Production, Transport and Storage*. New York: CRC Press, 2009, pp. 38–61.
- [6] K. Pornmai, N. Arthiwet, N. Rueangjitt, H. Sekiguchi, and S. Chavadej, “Synthesis gas production by combined reforming of CO<sub>2</sub>-containing natural gas with steam and partial oxidation in a multistage gliding arc discharge system,” *Industrial & Engineering Chemistry Research*, vol. 53, pp. 11891–11900, Jul. 2014.
- [7] N. Rueangjitt, T. Sreethawong, S. Chavadej, and H. Sekiguchi, “Plasma-catalytic reforming of methane in AC microsized gliding arc discharge: Effects of input power, reactor thickness, and catalyst existence,” *Chemical Engineering Journal*, vol. 155, pp. 874–880, Oct. 2009.
- [8] Y. C. Yang, B. J. Lee, and Y. N. Chun, “Characteristics of methane reforming using gliding arc reactor,” *Energy*, vol. 34, pp. 172–177, Jan. 2009.
- [9] Y. N. Chun, Y. C. Yang, and K. Yoshikawa, “Hydrogen generation from biogas reforming using a gliding arc plasma-catalyst reformer,” *Catalyst Today*, vol. 148, pp. 283–289, Oct. 2009.
- [10] Z. A. Allah and J. C. Whitehead, “Plasma-catalytic dry reforming of methane in an atmospheric pressure AC gliding arc discharge,” *Catalysis Today*, vol. 256, pp. 76–79, May. 2015.